Science in China Series E: Technological Sciences

www.scichina.com
tech.scichina.com
www.springerlink.com

Study of lubrication behavior of pure water for hydrophobic friction pair

MA ZhiZuo, ZHANG ChenHui†, LIU ShuHai, LUO JianBin, LU XinChun & WEN ShiZhu

State Key Laboratory of Tribology, Tsinghua University, Beijing 100084, China

The perfluorooctyltrichlorosilane molecular layer was self-assembled on glass plate. The tribological properties of the molecular layer in water were studied with the method of ball on disk. An interesting phenomenon was found that low friction coefficients of 0.02—0.08 were obtained when the friction pair was lubricated with only a water droplet. Whereas, when the friction pair was encircled with large amount of water or fully immersed in water, the friction coefficient was higher than that under a droplet lubrication. A mechanism of water droplet lubrication was proposed that the surface tension caused by the solid-liquid-air three-phase interface makes water molecules enter into the contact zone, which separates the two friction surfaces and provides a low friction coefficient. However, water film can hardly form when more water encircles the friction pair, due to the attraction between water molecules.

hydrophobic surface, water lubrication, friction coefficient

1 Introduction

Water-based lubrication has been paid more attention than ever by scientists and engineers because of its advantages such as environment friendly, uninflammable, and excellent cooling performance. At present, water is mainly used as lubricants for ceramic friction pairs due to electrostatic double layer effect and tribochemistry effect with silica[1−6], and also for polymer friction pairs due to the their elastic deformation for forming lubricating film[7,8]. However, the water can hardly form film in elastohydrodynamic contact due to its low viscosity and low pressure viscosity coefficient, which makes water hardly be used as lubricant in elastohydrodynamic contact. Many surface modifying arts (for example, coated with DLC, grafted with self-assembly monolayer with different chemical groups, etc) were used to change the interaction between water and friction pairs to improve the applied possibility of water lubrication in many fields. A lot of studies have been done by investigating the interaction between self-assembling molecular brushes or polymer and water through experimental and molecular dynamics methods to discover the mechanism of water lubrication. Klein's researches[9,10] realized super lower friction coefficients about 0.0006—0.001 with polyelectrolyte brushes in water. Spencer et al.[11−13] used poly(*L*-lysine)-g-poly(ethylene glycol) as additive to improve the lubricating properties of water for metal-oxide-based tribo- systems. Consta et al.[14] studied an ultra-thin water film confined between two moving surfaces using langevin molecular dynamics and found that the hydrophilic surfaces exhibited a lower friction than the hydrophobic ones. Jiang et al.[15] studied the nanoscale friction between alkyl monolayers immersed in liquid solvents using nonequilibrium molecular dynamics simulations and the results showed that friction was dependent not only on surface hydrophobicity, but also on solvent polarity. Beside that, Suzuki et al.[16] studied the load-carrying capacity and friction force of a water droplet about 8 μL confined between two hydrophobic surfaces

Received September 2, 2008; accepted December 2, 2008
doi: 10.1007/s11431-009-0137-x
†Corresponding author (email: chzhang@mail.tsinghua.edu.cn)
Supported by National Natural Science Foundation of China (Grant Nos. 50605034 and 50721004) and National Basic Research Program of China ("973" Program) (Grant No. 2007CB607604)

Citation: Ma Z Z, Zhang C H, Liu S H, et al. Study of lubrication behavior of pure water for hydrophobic friction pair. Sci China Ser E-Tech Sci, 2009, 52(11): 3128—3134, doi: 10.1007/s11431-009-0137-x

and obtained a low friction force at low shear velocity. In addition, the influence of adsorbed water on the tribological performance was also studied by some researchers[17,18]. Most of the above studies focused on the effect of the surface characters on the water film forming capability and the interaction between water molecular and chemical groups. Although the water lubrication has been studied for a long time, problems such as whether water can form a lubricating film in elastohydrodynamic contact remains unsolved. In this paper, the behavior of water between two hydrophobic surfaces was studied, and an interesting phenomenon was presented.

2 Experimental details

In this paper, 1H, 1H, 2H, 2H-Perfluorooctyltrichlorosilane (C8F) self-assembling layer was prepared on glass plates with size of 24 mm×24 mm to obtain the hydrophobic surface. Before the cultivation of the self-assembling layer, two pre-treatments for the glass surface, cleaning and hydroxylating, were taken. First, all substrates were ultralsonically cleaned in acetone and chloroform for ten minutes, respectively to remove any organic contamination on the glass surface. After being flushed with deionized water (resistivity＞18 MΩ·cm), these cleaned substrates were dipped in piranha solution, which was a mixture of hydrogen peroxide and concentrated sulfuric acid with the volume ratio of 3∶7. The temperature was controlled at 90℃ by water bathing, and the reaction time was 60 min. Then, these hydroxylated substrates were cleaned with deionized water and dried with dry nitrogen flow. After pre-treatments, these substrates were dipped in the solution of toluene and 1H, 1H, 2H, 2H-Perfluorooctyltrichlorosilane (C8F) (Aldrich, USA) for the growth of the silicane self-assembling layer. After 5 h, these samples were taken out from the solution and then ultralsonically cleaned with toluene to remove the physical adsorbed molecules. Finally, these specimens were dried with nitrogen flow and then were placed into an enclosed drying apparatus waiting for the surface analysis and friction tests.

To characterize the linkage between glass and C8F, XPS analysis was performed on a PHE-5100X instrument. The morphology of glasses, self-assembling layer and their tribological counter part, a silicon nitride ball were investigated by atomic force microscope (Nanoscope IIIa Multimode). All provided morphology images were recorded using a contact mode with silicon cantilever tips (Park Scientific, CA). They are shown in height mode without any image processing except flattening. Analysis of the AFM images was carried out using Nanoscope III software (version 5.12r2).

The static contact angle between water and the glass plates with and without the self-assembling layer were measured by an optical contact angle meter (JC2000A, China). The volume of the water drop was about two micro liters. Three samples with the same treatment were used for the measurement, and the measurements were carried out on at three different positions for each sample. The reported values in this paper are averages of these measurements.

Friction tests were performed on UMT-2 (CETR, USA) tribometer with a mode of ball-on-disk. The upper specimen was a Si_3N_4 ball with a diameter of 4 mm. The rotary speed of the samples was 30 r/min, providing a linear sliding speed of 21.2 mm·s^{-1} at a track diameter of 13.5 mm. The Si_3N_4 ball was cleaned ultrasonically with acetone before the test and a new ball was used for each test. In the study, this kind Si_3N_4 ball offered a hydrophobic surface for the tribology test. The normal load of 0.4 N gave a maximal contact pressure approximately 330 MPa (calculated using the Hertzian Contact Model). All tests were performed at the temperature about 26℃ and the relative humidity about 50%.

In this work, the friction tests were carried out under dry friction, droplet lubrication and full water immersion conditions separately, as schematically described in Figure 1.

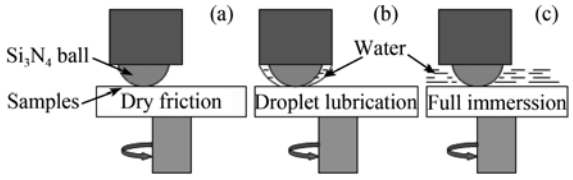

Figure 1 Schematics of the three friction conditions. (a) Dry friction; (b) droplet lubrication; (c) full water immersion.

3 Results

3.1 Surface characteristics

Figure 2 shows the XPS spectra of the surface of bare glass plate and glass plate modified with C8F self-assembling layer. The peaks of O, C, Si, Ca and Mg in Figure 2(a) came from the composition of glass, while the peak of fluorine in Figure 2(b) came from the $-CF_3$ group of the C8F molecules, indicating that C8F layer has grown on the glass plate surface.

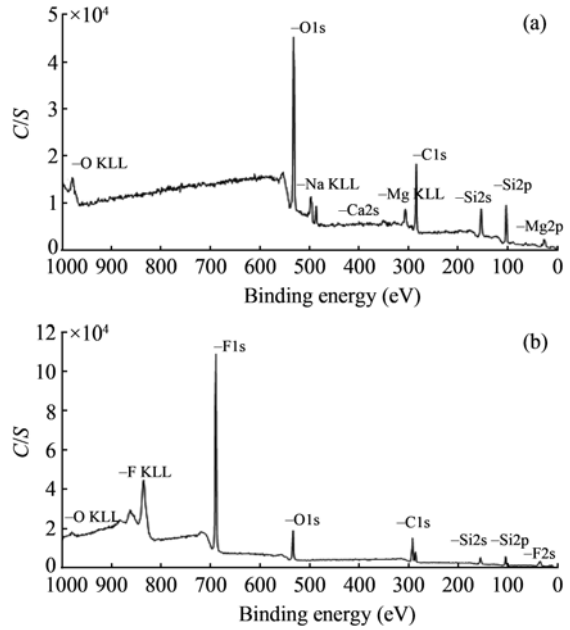

Figure 2 XPS curves of (a) bare glass plate and (b) glass plate modified with C8F.

The average contact angles of water on bare glass plate and C8F self-assembling layer are 22° and 104°, respectively and their typical images are shown in Figure 3. The interaction energy between specimens and deionized water can be calculated according to Young equation:

$$\gamma(1+\cos\theta)=\Delta W_{\mathrm{SLV}} \tag{1}$$

where γ is the water-air energy and its value is about 0.072 N/m, θ is the experimental contact angle, ΔW_{SLV} is the energy per unit area at the interface between the solid and liquid surfaces in room environmental. According to the above equation, the calculated ΔW_{SLV} between water and bare glass is about 138.7 mN/m while ΔW_{SLV} between water and C8F layer is about 54.6 mN/m.

Figure 4 shows the three dimensional topographies of the Si_3N_4 ball, the bare glass plate and the C8F self-assembling layer. The scanning scope for all the specimens is all 5 μm×5 μm. It should be noted that the

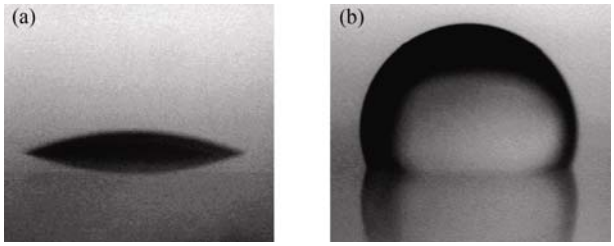

Figure 3 Contact angle images of water drop on (a) bare glass plate and (b) C8F layer.

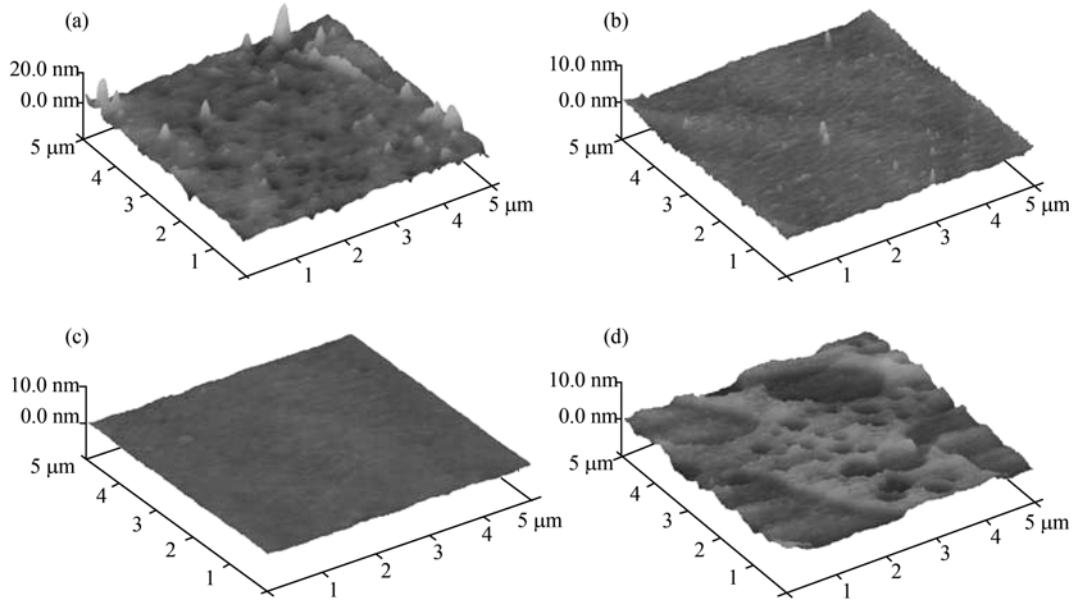

Figure 4 AFM images of (a) the Si_3N_4 ball, (b) the bare glass, (c) glass with C8F self-assembling layer and (d) glass with C8F self-assembling layer after being immersed in water for 30 min.

images of the Si_3N_4 ball and the glass (Figures 4(a) and (b)) were obtained in atmosphere. While in order to obtain clear signals, the images of C8F layer (Figures 4(c) and (d)) were captured in deionized water environment.

As shown in Figure 4(a), the surface of the Si_3N_4 ball is full of micro pits and micro bulges, and the root mean square roughness is about 2 nm. The topography of the glass shown in Figure 4(b) is smooth and its roughness is 0.33 nm. After the glass surface was covered by C8F layer, its roughness reduced to 0.18 nm. However, the roughness increased to 0.8 nm after the sample with C8F layer was immersed in water for about 30 min. And some pin holes can be found on the surface as shown in Figure 4(d). The degradation of C8F layer in water is attributed to the hydrolysis of slicane[19,20].

3.2 Friction tests

Figure 5 shows the friction coefficients of bare glass against the Si_3N_4 ball under dry friction and full water immersion conditions. It can be seen that the friction coefficient quickly increased from the initial value 0.6 to 0.8 and remained at that value till the end of the test whatever the friction with water lubrication or not.

The friction coefficients of the glass with C8F layer against the Si_3N_4 ball under dry friction and droplet lubrication (volumes: 5 μL, 10 μL) are shown in Figure 6. Under dry friction, the friction coefficient increased rapidly from about 0.18 to 0.8 which was similar to the friction coefficient of bare glass in Figure 5. Under water droplet lubrication with the water volumes of 5 and 10 μL, lower friction coefficients appeared in the beginning and then the friction coefficients increased to about 0.8 at the end of the tests.

When increasing the volume of the droplet to 20 μL, an interesting phenomenon was found that the friction coefficient reduced to 0.04 after running a short-time

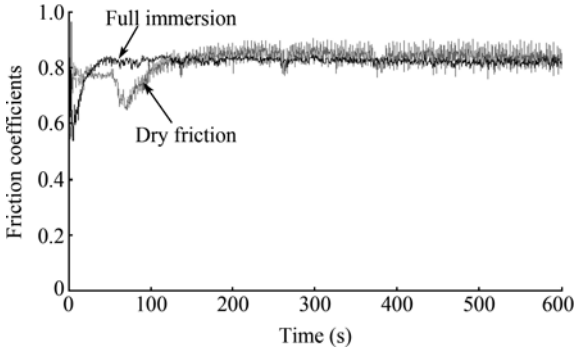

Figure 5 Friction coefficients curves of bare glass against Si_3N_4 ball under dry friction and full water immersion.

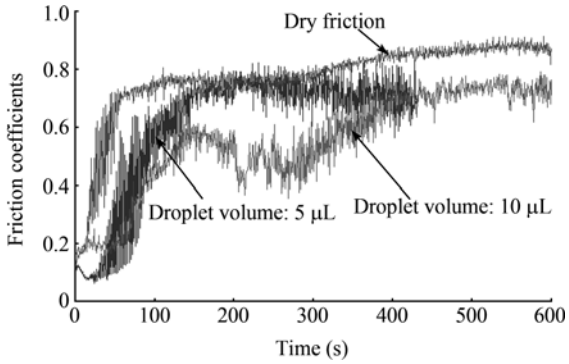

Figure 6 Friction coefficients curves of the glass with C8F layer against Si_3N_4 ball under dry friction and water droplet lubrication with water volumes of 5 and 10 μL, respectively.

and kept constant till the end of the test, as shown in Figure 7. With the water volume varying from 20 to 200 μL, the friction coefficient fluctuated from 0.02 to 0.08, without obvious dependence on the water volume (Figure 7).

However, with increasing the droplet volume continuously, the friction coefficient changed. When the droplet volume increased to 250 μL, the friction coefficients rose up slowly from the lower level around 0.16 to a higher level about 0.8 during the tests, as shown in Figure 8. For the droplet volume of 300 μL, the friction

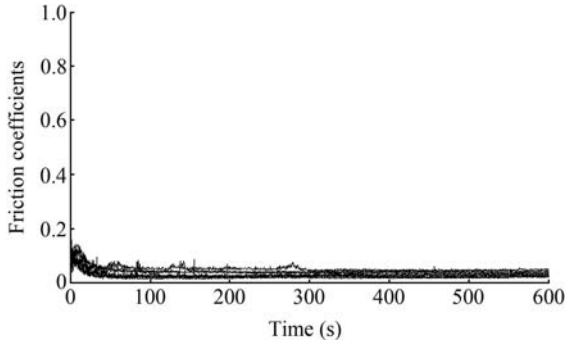

Figure 7 Friction coefficient curves of C8F against Si_3N_4 ball under water droplet lubrication (volumes: 20, 30, 40, 50, 75, 100, 150, 200 μL).

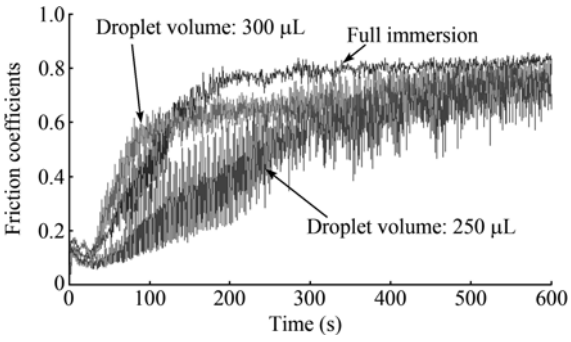

Figure 8 Friction coefficients curves of C8F modified glass plate against Si_3N_4 ball under water droplet lubrication (volumes: 250, 300 μL) and full immersion.

coefficient increased quickly as compared with the case of 250 μL. The friction coefficient curve is similar to that in the case of full immersion, as shown in Figure 8. These interesting results indicate that the water droplet with appropriate volume could act as a lubricant to separate the two surfaces effectively.

4 Discussion

As described in the previous section, the friction coefficient of glass with C8F layer shows quite different in different lubricating conditions. Figure 9 shows the dependence of friction coefficient on the volume of water droplet. For comparison, the friction coefficients of the bare glass under dry friction and water lubrication are also included.

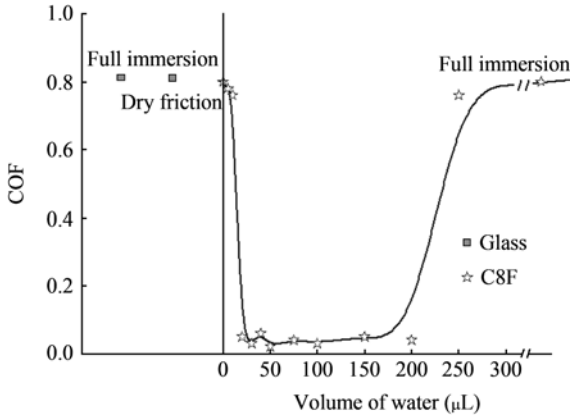

Figure 9 Final values of friction coefficients between the hydrophobic C8F layer and the hydrophobic Si_3N_4 ball under water lubrication with series volumes.

The shape of the curve shown in Figure 9 appeared like a capital "U". At the left part, the friction coefficients of the C8F layer under dry friction are similar to those of the bare glass. This can be attributed to the low strength of C8F layer. The C8F layer was worn out at the beginning of the test under the contact pressure of 330 MPa. And then, the Si_3N_4 ball contacted the glass substrate directly. When the volume of water was smaller than 10 μL, the friction coefficients were equivalent to those in dry friction, meaning that water molecules could not enter into the contact zone to act as lubricant in such conditions. At the right part of the curve, high friction coefficients were obtained under full immersion or water droplet with a volume lager than 200 μL. In such cases, it was supposed that water could not enter into the contact zone too although the contact region was encircled by water. In other words, water could not form a film to lubricate the friction pairs. However, an interesting phenomenon appeared at the bottom of "U" when a proper amount of water was added to the contact zone. In the experiments, low friction coefficient at the order of 10^{-2} was obtained when the water volume in the range of 20 to 200 μL. A reasonable explanation for the low friction is that a thin water film forms in the contact area.

To investigate the role of the water in the contact area, the evolution of the water around the friction pair was recorded by a video camera, and some typical frames are shown in Figure 10. When the volume of water droplet was 10 μL, the small water droplet accumulated at the exit of the contact area, and no water can be seen in the entrance. As a result, the water can not enter into the contact zone to lubricate the friction pair. When the droplet volume increased, the water was sufficient to surround the Si_3N_4 ball as shown in Figure 10(a), and a three-phase interface of solid-liquid-gas was formed at the entrance of the contact area. With further increasing the droplet volume, redundant water gathered at the exit of the contact area and went along with the ball to form a tail, as shown in Figure 10(b). In such a case, the friction coefficient decreased to a value in the range of 0.02

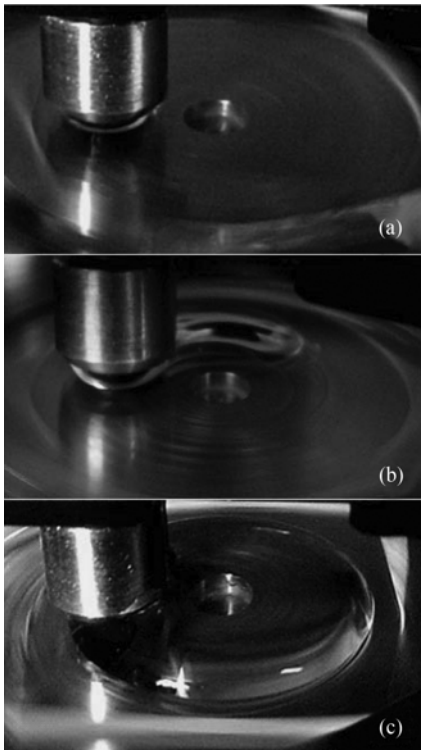

Figure 10 Photographs of water shape close to the contact zone under (a) 40 μL, (b)150 μL, (c) 450 μL immersion.

to 0.08. However, when the droplet volume was big enough (>200 μL), the tail was so long that the entrance reached the end of the tail to form a closed water circle and the friction coefficient increased to about 0.8 rapidly. In fact, when the volume of water was bigger than 250 μL in our tests, the droplet would change into a pool that more water would surround the friction pair like the condition of full immersion, as shown in Figure 10(c).

Based on the above observation, a simple model attempting to illustrate the lubrication mechanism of water film forming under droplet lubrication was proposed, as shown in Figure11.

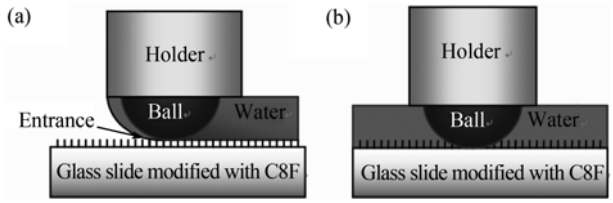

Figure 11 Mechanism of water film (a) forming under droplet lubrication and (b) its failure under full immersion.

When the water was sufficient, a meniscus was formed at the entrance of the contact zone due to the interaction between air, water, C8F layer and the upper ball, as shown in Figure 11(a). Some water molecules were compelled into the contact area by the surface tension and formed a thin water layer. Due to the lower adhesion between the water molecule and the C8F molecule, the water layer adhered to the ball surface and went along with the ball together. In such case, the friction force comes mainly from the van der Waals attraction between the water molecules and the C8F molecules. The proposed model of water droplet lubrication is based on a hypothesis that the water film in the contact zone can support the applied load. The load carrying capability of the droplet confined to the two hydrophobic surfaces can be calculated by multiplying the Laplace pressure by solid-liquid interfacial area as follows[21,22]:

$$w = \gamma\left(-\frac{2\cos\theta}{d}+\frac{1}{R}\right)\pi R^2, \qquad (2)$$

where d is the distance between the two separated surfaces, R is the radius of the droplet, γ is the surface tension of water (0.072 N/m), and θ is the contact angle of the water droplet on the sample surface. Under the applied normal load, the spherical cap of the ball deformed elastically and the radius of the contact area "b" is about 22 μm. Only the water confined to this contact zone plays an important role to support the normal load despite other water surrounding the ball. So in this study, it is reasonable to set the value of "R" in the order of "b", that is in the range of 20—100 μm. Under the normal load, the water droplet should be deformed and a larger contact angle nearly 180° should be obtained. Considering the friction coefficient in the order of 10^{-2}, the lubricating state in the tests should be mixture lubrication. It means that the film thickness of water in the contact area is similar to the surface roughness. Then, a separation distance "d" less than 3 nm is reasonable. Substituting R of 40 μm, θ of 180°, d of 2 nm into eq. (2), a supporting force of 0.36 N can be achieved, which is quite similar to the normal load of 0.4 N applied in the experiments. As a result, the two surfaces were separated by the water layer. And a lower friction coefficient was obtained due to the low adhesion force between the water layer and the hydrophobic C8F layer.

When the friction pair was surrounded by large amount of water, the simple model for the lubrication mechanism would be described in Figure 11(b). The three-phase interface at the entrance of contact area is substituted by the solid-liquid two-phase interface. There is no surface tension to force the water molecules to enter into the contact area. The water molecules incline to leave the contact area due to the cohesive force among water molecules and the weak affinity between the water molecules and the hydrophobic surfaces. As a result, the ball contacts with the C8F film directly. The C8F film is worn out very quickly due to its poor strength. The high friction coefficient of 0.8 comes from the direct contact between the ball and glass substrate.

According to above analysis, it is the key for water droplet lubrication that the surface tension comes from the solid-liquid-air three-phase interface. To verify our supposition, additional experiment was carried out. When a low friction coefficient was achieved during the water droplet lubrication test, an extra water droplet with volume of 50 μL was dropped ahead the entrance. Figure 12 shows the variation of the friction coefficient during the test. With the specimen rotating, the extra water droplet met with the friction pair and merged with the water at the entrance of contact area. When the mergence happened, the three-phase-interface disappeared and an increase of friction coefficient was found simultaneously. Rapidly, the extra water at the entrance

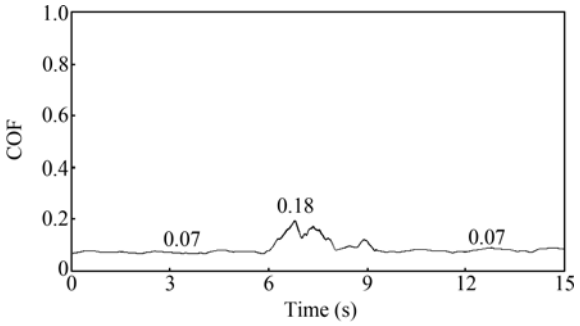

Figure 12 Friction coefficients before and after an extra droplet merging with the water at the entrance.

moved to exit of the contact area, forming a part of the water tail. The three-phase-interface reappeared and the friction coefficient decreased to the original level. The experiment result confirmed that the solid-liquid-gas plays an important role in water droplet lubrication, and the mechanism of water droplet lubrication proposed above has been proved.

5 Conclusion

In this work, the tribological behavior between two hydrophobic surfaces with water lubrication has been investigated by the tribometer UMT-2. Low friction coefficients in the range from 0.02 to 0.08 were achieved when the hydrophobic friction pair was lubricated by a water droplet of proper volume. However, high friction coefficient of 0.8 was obtained in the cases where the friction pair was encircled by large amount of water or the friction pair was immersed in a water pool. It was considered that a thin water film can be formed in the contact region to separate the two sliding surfaces under droplet lubrication due to the surface tension at the solid-liquid-air three-phase interface. Such a water film can support the normal load and provide a low friction coefficient. Under full immersion or the friction pair was encircled by large amount of water, the attraction among water molecules themselves and the low affinity between the water molecules and the surface would lead the water molecules to escape from the contact zone, resulting in the direct contact between the two sliding surfaces. A conclusion can be derived that the solid-liquid-air three-phase interface is the key for achieving low friction in water droplet lubrication.

1 Tomizawa H, Fischer T E. Friction and wear of silicon nitride and silicon carbide in water: Hydrodynamic lubrication at low sliding velocity obtained by tribochemical wear. Tribol T, 1987, 30(1): 41－46
2 Honda F, Saito T. Tribochemical characterization of the lubrication film at the Si_3N_4/Si_3N_4 interface sliding in aqueous solutions. Appl Sur Sci, 1996, 92(1-4): 651－655
3 Xu J, Kato K, Hirayama T. The transition of wear mode during the running-in process of silicon nitride sliding in water. Wear,1997, 205(1-2): 55－63
4 Xu J G, Kato K. Formation of tribochemical layer of ceramics sliding in water and its role for low friction. Wear, 2000, 245(1-2): 61－75
5 Jordi L, Iliev C, Fischer T E. Lubrication of silicon nitride and silicon carbide by water: Running in, wear and operation of sliding bearings. Tribol Lett, 2004, 17(3): 13－20
6 Kalin M, Novak S, Vizintin J. Surface charge as a new concept for boundary lubrication of ceramics with water. J Phys D-Appl Phys, 2006, 39(15): 3138－3149
7 Yao J Q, Blanchet T A, Murphy D J, et al. Effect of fluid absorption on the wear resistance of UHMWPE orthopedic bearing surfaces. Wear, 2003, 255(2): 1113－1120
8 Vicente D J, Stokes Jr, Spikes H A. Lubrication properties of non-adsorbing polymer solutions in soft elastohydrodynamic (EHD) contacts. Tribol Int, 2005, 38(5): 515－526
9 Raviv U, Giasson S, Kampf N, et al. Lubrication by charged polymers. Nature, 2003, 425(6954): 163－165
10 Briscoe W H, Titmuss S, Tiberg F, et al. Boundary lubrication under water. Nature, 2006, 444(7116): 191－194
11 Lee S, Müller M T, Ratoi-Salagean M, et al. Boundary lubrication of oxide surfaces by poly(*L*-lysine)-g-poly(ethylene glycol) (PLL-g-PEG) in aqueous media. Tribol Lett, 2003, 15(3): 231－239
12 Müller M T, Yan X P, Lee S, et al. Lubrication properties of a brush-like copolymer as a function of the amount of solvent absorbed within the brush. Macromolecules, 2005, 38(13): 5706－5713
13 Müller M T, Lee S, Spikes H A, et al. The influence of molecular architecture on the macroscopic lubrication properties of the brush-like co-polyelectrolyte poly(*L*-lysine)-g-poly(ethylene glycol) (PLL-g-PEG) adsorbed on oxide surfaces. Tribol Lett, 2003, 15(4): 395－405
14 Paliy M, Braun O M, Consta S. The friction properties of an ultrathin confined water film. Tribol Lett, 2006, 23(1): 7－14
15 Zhang L Z, Jiang S Y. Molecular simulation study of nanoscale friction between alkyl monolayers on Si(111) immersed in solvents. J Chem Phys, 2003, 119(2): 765－770
16 Suzuki K, Uyeda Y. Load-carrying capacity and friction characteristics of a water droplet on hydrophobic surfaces. Tribol Lett, 2003, 15(2): 77－82
17 Patton S T, Bhushan B. Environmental effects on the streaming mode performance of metal evaporated and metal particle tapes. IEEE T Magn,1997, 33(4): 2513－2530
18 Patton S T, Eapen K C, Zabinski J S. Effects of adsorbed water and sample aging in air on the μN level adhesion force between Si(100) and silicon nitride. Tribol Int, 2001, 34(7): 481－491
19 Ismael D P, Mónica L, Fernando T, et al. Interaction of water with self-assembled monolayer of alkylsilanes on mica. Langmuir, 2004, 20(4): 1284－1290
20 Zhang L J, Zhang Y, Zhang R J, et al. *In situ* AFM investigations on degration of self-assembled monolayer on mica: Effect of humidity. Colloid Surf A, 2007, 293(1-3): 195－200
21 Israelachvili J. Intemolecular and Surface Forces. 2nd ed. London: Academic Press,1992. 330－334
22 Suzuki K. Flow resistance of a liquid droplet confined between two hydrophobic surfaces. Microsyst Technol, 2005, 11(8-10): 1107－1114